Stationary Phase Method Application for the Analysis of Radiation of Complex 3-D Conducting Structures

Olga M. Conde, Jesús Pérez, and Manuel Felipe Cátedra

***Abstract*—The *Stationary Phase Method* is used to calculate the radiation pattern of antennas on complex structures. Physical optics (PO) approximation has been applied for the induced currents. The problem is stated directly over the parametric surfaces used to model the geometry and no translation of geometrical formats is required. The integral comes from the contribution of certain points on the surface (specular, boundary and vertices) where the phase term of the integrand presents a stationary behavior. In general, the asymptotic integration behaves similar to the numerical one but being more efficient in execution time than the latter.**

***Index Terms*—Asymtotic methods, complex structures, parometric surfaces, physical optics, radiation, stationary phase method.**

I. Introduction

THE analysis of radiation of on-board antennas is still a problem when the structure presents arbitrary shapes. A numerical solution is essential in order to avoid the always cumbersome and expensive trial-and-error measurement process in anechoic chambers. Appropriate solutions to the problem should combine the knowledge of two different topics: 1) the geometrical design world and 2) the electromagnetic (EM) analysis field. In the first case, a suitable and accurate representation of the body should be applied while keeping the required storage requirements as low as possible. For the present approach, this is achieved by using parametric surfaces called nonuniform rational b-splines (NURBS) [1], [23].

The radiation problem is tackled by establishing the equivalent current problem. Under the operating conditions, the electrical size of the structure reaches hundreds or thousands of λ^2 making the analysis by the sampling of the induced current economically unaffordable. Evidently, the technique to be applied should be chosen from the group of high-frequency techniques. Physical optics (PO) [2], [3] has revealed itself as one of the more appropriate techniques [4], and because of this it has been selected for the case we shall deal with. PO approaches the induced current as the one attributed only to the impressed field. Afterwards, in order to obtain the radiated field this current has to be integrated. If a typical numerical technique such as the Gauss quadrature [5] is applied, the same problem of inefficiency arises owing to the rapid oscillation of the integrand's phase.

The stationary phase method (SPM) is a mathematical approach that takes advantage of the rapidly varying integrand's phase [6]–[16]. The solution to the integral is given by the contribution of certain points distributed over the surface of the body. If we look carefully through the physical meaning of these contributions, they resemble in same way the typical contribution points in traditional asymptotic techniques such as geometrical optics and geometrical theory of diffraction/uniform theory of diffraction (GO/UTD) [17]. This fact seems logical as we are dealing with a high-frequency approximation of the electromagnetic (EM) problem.

Several have been the applications of the SPM in the scope of EM analysis. To the author's knowledge, most of them are related to integration in one dimension and very little information has been obtained regarding two-dimensional (2-D) integral problems. In one of the earliest applications [18], a modified SPM is applied to compute the far-field radiation patterns of paraboloid reflector antennas. In [19], the far field of a pyramidal-horn antenna is obtained numerically in one-dimension (1-D) and asymptotically in the other. Later, Ikuno in [20] applied the PO approach in the evaluation of the scattered field from a 2-D nonconvex scatterer taking into account only the contribution of points of the first kind. More recently, and with the collaboration of Nishimoto [21], he has extended the combination PO/SPM to the scattering analysis of smooth three-dimensional (3-D) objects described in terms of polar coordinates $\vec{r}(\theta, \varphi)$. Again, only stationary points of first kind are included in the analysis. In [21], they also advised about the difficulty of finding a uniform asymptotic evaluation for double integrals. In [22], Nakano *et al*.employed the SPM to integrate the resulting currents for printed wire antennas to obtain the radiation pattern at a far-field point.

Concerning the combination of geometrical modeling with the SPM, good results were achieved in [23] where the analysis of the scattering field and radar cross section (RCS) of complex targets were studied. In that case, the impressed field was a planewave and the observation directions were located along the monostatic direction. In current work, the SPM has been reformulated and it has been used to see how it performs with regard to a radiation problem. The incident field is now a spherical wavefront, the source is positioned over the surface of the structure, and the observation direction can be any given direction, in order to calculate the radiation pattern.

Manuscript received October 2, 1998; revised July 27, 2000.

This work has been supported by C.Y.C.I.T. under a F.P.U. grant, CYCIT Projects IN94-0108, TIC96-0653, and DES96-2048.

O. M. Conde is with the Department Tecnología Electrónica e Ingeniería de Sistemas y Automática. Universidad de Cantabria, 39005 Santander, Spain.

J. Pérez and M. F. Cátedra are with the Department of Teoría de la Señal y Comunicaciones, Universidad de Alcalá, Escuela Politécnica Ctra. Madrid-Barcelona, Madrid, Spain. (e-mail: felipe.catedra@uah.es).

Publisher Item Identifier S 0018-926X(01)03186-6.

II. PO Integral and the SPM

The integral that accounts for the radiated field when the on-board antenna generates the incident wave is found after the formulation of the Stratton-Chu integral equations [24]. The radiated field at an arbitrary point $\vec{r}$ is provided in terms of tangential and normal components of the total fields $\vec{E}, \vec{H}$ on the surface of the body. Field vectors are time harmonic with dependence on $e^{j\omega t}$.

The incident wavefront is assumed spherical, i.e., the antenna radiates fields with spheres as surfaces of constant phase. Any available antenna could be modeled as a set of infinitesimal electric or magnetic dipoles considered as the typical spherical sources. The infinitesimal dipoles of the antenna model radiate under far-field observation [3]. The impressed electric field can be represented by

$$\vec{E}_I(\vec{r}') = \vec{E}_0(\vec{r}')e^{-jkd} \quad d = |\vec{k}_I| = |\vec{r}' - \vec{r}_{\text{SOURCE}}| \tag{1}$$

where

- $\vec{E}_0(\vec{r}')$ electric field at the sampling point due to the infinitesimal source once the phase term has been extracted;
- $\vec{r}'$ surface point where the current is determined;
- $\vec{r}_{\text{SOURCE}}$ represents the position coordinates of the source dipole in the absolute reference system;
- k propagation constant (the wavenumber) which becomes larger in the range of high-frequency analysis;
- $\hat{k}_I$ is the unit incident wave direction.

The final expression for the radiated field in the observation direction $\hat{k}_S$ becomes

$$\vec{E}_S(\vec{r}) = \frac{-j}{\lambda}\frac{e^{-jk|\vec{r}|}}{|\vec{r}|} \cdot \int_{S_{\text{ILLUMINATED}}} \frac{[\hat{k}_S \times [(\vec{E}_0(\vec{r}') \times \hat{k}_I) \times \hat{n}]] \times \hat{k}_S}{d} \cdot e^{jk(\hat{k}_S \cdot \vec{r}' - d)}\, ds' \tag{2}$$

In the integrand of (2), the fractional factor represents the amplitude variation over the surface and the exponential term is related to the optical path [6], [7]. When the shape of the surface is smooth, the variation of parameters $\hat{n}$ (normal vector to the surface), $\hat{k}_I$ (unit incidence direction) and d (distance source-sampling point) is also smooth giving rise to a slowly varying amplitude. On the other hand, the variation of the optical path is related to the target size in terms of wavelengths; if this size is in the order of several λ's, the exponential $e^{jk(\hat{k}_S \cdot \vec{r}' - d)}$ oscillates very quickly. The phase exhibits maximum or minimum values related to the length of the optical path followed by the field. As the amplitude variation is smooth, terms with oscillating phase and similar amplitude cancel each other in the integral summation except in the area where the phase remains roughly constant, i.e., the stationary points.

The SPM is a mathematical procedure that solves integrals on the shape

$$I = \int_H g(\vec{x})e^{jkf(\vec{x})}\, dx_1\, dx_2 \cdots dx_n \qquad \vec{x} = (x_1, x_2, \cdots, x_n) \tag{3}$$

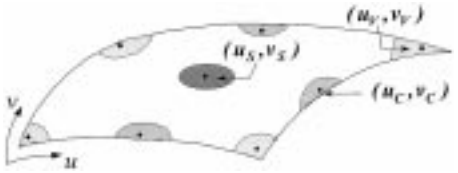

Fig. 1. Localization of the critical points over the Bézier surface.

where

- H integration domain;
- $\vec{x}$ n-dimensional variable that underlies the problem, the two independent variables (u, v) that define each Bézier surface;
- $g(\vec{x})$, $f(\vec{x})$ slowing analytical functions in the integration domain;
- k real factor with a large value.

Similarities can be extracted from integrals (2) and (3), functions $g(\vec{x})$ and $f(\vec{x})$ can be clearly identified: $H = S_{\text{ILLUMINATED}}$, $n = 2$ and $dx_1 dx_2 = du dv = ds' = |\vec{r}'_u \times \vec{r}'_v|$.

III. Contributions to the PO Integral

From the mathematical point of view, the SPM solves the integral following paths of constant level where the phase has a stationary behavior [8]. The phase term is expanded in Taylor series around the stationary points. In the end, the solution is cast as a descending power series in the parameter k. The principal contributions to the double integral come from a small arbitrary area of certain points, called critical points of the integral, located internally or on the boundary of the integration domain [6], [9].

In the on-board antenna application, each parametric surface contributes to the integral by means of three different kinds of critical points [6], [10], [12], see Fig. 1.

A. Internal Critical Points

These points present a stationary behavior in the phase for both dimensions of the Bézier surface u and v. The previous statement is translated, from a mathematical point of view, into the system of two nonlinear equations (4). The solution of the system gives rise to the parametric values of the stationary points (u_S, v_S) involved in the analysis

$$\begin{cases} f_u(u_S, v_S) = 0 \\ f_v(u_S, v_S) = 0 \end{cases} \Rightarrow \begin{cases} \left.\dfrac{\partial f}{\partial u}\right|_{(u_S, v_S)} = 0 \\ \left.\dfrac{\partial f}{\partial v}\right|_{(u_S, v_S)} = 0 \end{cases} \Rightarrow \begin{cases} (\hat{k}_s - \hat{k}_i) \cdot \vec{r}_u|_{(u_S, v_S)} = 0 \\ (\hat{k}_s - \hat{k}_i) \cdot \vec{r}_v|_{(u_S, v_S)} = 0. \end{cases} \tag{4}$$

A trivial solution of the system (4) is the case of coincident incidence and observation directions $\hat{k}_S = \hat{k}_I$, $\gamma = a\cos(\hat{k}_S \cdot \hat{k}_I) = 0$. The points that accomplish with this condition are those where the observation direction is hidden by the structure. The solution (u_S, v_S) is found after the minimization of a

function $s(u,v)$ that is formulated in terms of geometrical parameters as

$$\begin{aligned} s(u,v) &= s_1(u,v) + s_2(u,v) \\ &= \{[\vec{k}_I \cdot \vec{k}_I]^2 - |\vec{k}_I|[\hat{k}_S \cdot \vec{k}_I]\} \\ &\quad + \{[\vec{k}_I \cdot \vec{k}_I]^2 - [\hat{k}_S \cdot \vec{k}_I]^2\} \\ \vec{k}_I(u,v) &= \vec{r}'(u,v) - \vec{r}_{\mathrm{SOURCE}}. \end{aligned} \tag{5}$$

Other solutions of (4) are also the specular points that accomplish with the Snell's Law. These points are found after the generalization of Fermat's Principle by the minimization of a distance function [3], [25], [26]. This function is composed of two partial lengths: d_1 and d_2. The term d_1 accounts for the path from the source to the surface point whereas d_2 is the distance between the surface point and a plane perpendicular to the observation direction located at a distance much greater than the structure dimension, d_{INF}

$$\begin{aligned} d(u,v) &= d_1(u,v) + d_2(u,v) \\ &= \{|\vec{r}'(u,v) - \vec{r}_{\mathrm{SOURCE}}|\} + \{d_{INF} - \hat{k}_S \cdot \vec{r}'(u,v)\}. \end{aligned} \tag{6}$$

The minimization of $d(u,v)$ takes us to the Geometric Optics solution for reflection points. In the minimization process of (5) and (6), a numerical algorithm based on the conjugate-gradient method [5] with the Polak–Ribiere formula is applied. Once the point location (u_S, v_S) is determined, the next step consists of calculating its contribution to the integral. The contribution depends on the characteristics of the phase function. The notation to be utilized is

$$\begin{aligned} \vec{g}^S &= \vec{g}(u_S, v_S), \quad f^S = f(u_S, v_S) \\ ds^S &= |\vec{r}_u^S \times \vec{r}_v^S| = \left| \frac{\partial \vec{r}}{\partial u} \times \frac{\partial \vec{r}}{\partial v} \right|_{(u_S, v_S)} \\ f_{uu}^S &= \left. \frac{\partial^2 f}{\partial u^2} \right|_{(u_S, v_S)}, \quad f_{uv}^S = \left. \frac{\partial^2 f}{\partial u \partial v} \right|_{(u_S, v_S)} \\ f_{vv}^S &= \left. \frac{\partial^2 f}{\partial v^2} \right|_{(u_S, v_S)}, \ldots, f_{vvv}^S = \left. \frac{\partial^3 f}{\partial v^3} \right|_{(u_S, v_S)}. \end{aligned} \tag{7}$$

When we face a simple isolated internal point that is nondegenerate and does not present any singularity, the following contribution is considered [6], [8], [10], [12]–[16]:

$$\begin{aligned} \vec{I}_S &= \frac{2\pi \vec{g}^S}{k} e^{jkf^S} \sqrt{\frac{1.0}{|f_{uu}^S f_{vv}^S - (f_{uv}^S)^2|}} e^{j(\pi/4)\sigma(\delta+1)} \, ds^S \\ &\Rightarrow \sigma = \mathrm{sign}(\mathrm{f_{vv}^S}) \\ &\quad \delta = \mathrm{sign}(\mathrm{f_{uu}^S f_{vv}^S - (f_{uv}^S)^2}) \\ \mathrm{sign(x)} &= \begin{cases} 1 & x \geq 0.0 \\ -1 & x < 0.0. \end{cases} \end{aligned} \tag{8}$$

Values σ and δ depend on whether the stationary point is a local minimum, a local maximum or a saddle point [9], [15]. Moreover, when the interior stationary point lies directly over one of the boundaries of the surface, the contribution is half of (8), [8], [12]–[15]. Additionally, as special cases we deal with the following singularities:

1) Degenerate stationary points where the Hessian matrix of f is singular $|f_{uu}^S f_{vv}^S - (f_{uv}^S)^2| = 0$. In this case, the contribution has a lower order in the parameter k, $O(k^{-(5/6)})$. The contribution for a squared domain as the parametric one is shown in [12], [29].
2) Internal stationary points located at a corner or vertex of the domain; different expressions [15], [29] are applied for the case of a local extremum $f_{uu}^S f_{vv}^S > (f_{uv}^S)^2$ (maximum or minimum) or a saddle-point $f_{uu}^S f_{vv}^S < (f_{uv}^S)^2$.

If several stationary points are found and provided they are well separated, their contributions must be added to account for the total effect of the structure. In general, internal critical points are assumed to be isolated, i.e., they are not close to each other and consequently their areas do not overlap. The fact of nonisolated critical points would reflect that we are dealing with a caustic line where the field comes from an infinite number of points on the surface and, therefore, the radiated field becomes infinite in the observation direction.

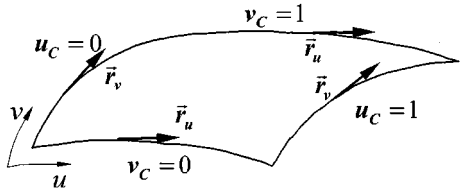

Fig. 2. Four boundaries of a parametric patch with their tangent vectors.

B. Critical Boundary Points

As their name reveals, they are positioned over the boundaries that circumvent the area of the parametric patch. For each Bézier surface four boundaries are analyzed: one for each line of the parametric square, Fig. 2: $u_c = 0.0$, $u_c = 1.0$, $v_c = 0.0$ and $v_c = 1.0$. At each boundary, one parametric coordinate is fixed and the phase function must exhibit a stationary behavior in the remaining coordinate

$$\begin{aligned} u_c = 0 \quad or \quad u_c = 1 &\Rightarrow \alpha = u_c \\ &\Rightarrow f_v(\alpha, v_c) = 0 \Rightarrow (\hat{k}_S - \hat{k}_I) \cdot \vec{r}_v|_{(\alpha, v_c)} = 0 \\ v_c = 0 \quad or \quad v_c = 1 &\Rightarrow \alpha = v_c \\ &\Rightarrow f_u(u_c, \alpha) = 0 \Rightarrow (\hat{k}_S - \hat{k}_I) \cdot \vec{r}_u|_{(u_c, \alpha)} = 0. \end{aligned} \tag{9}$$

From a physical point of view, this condition leads us to the Keller's cone, i.e., the incidence and observation directions $(\hat{k}_I, \hat{k}_S)$ make equal angles with the vector tangent to the boundary curve, $\vec{r}_u$ or $\vec{r}_v$. To find these critical points, instead of formulating a 1-D minimization process, a root finding algorithm is stated following a technique based on Brent's algorithm that combines root bracketing, bisection, and inverse quadratic interpolation [5]. This technique has been found faster than minimization, as well as more robust.

Before displaying the contributions for each point, the following remark in notation is made:

$$\begin{aligned} u_{CTE} = 0 \quad or \quad u_{CTE} = 1 &\Rightarrow \alpha = u, \quad \beta = v \\ \vec{g}^C = \vec{g}(u_{CTE}, v_C), &\quad f^C = f(u_{CTE}, v_C) \\ v_{CTE} = 0 \quad or \quad v_{CTE} = 1 &\Rightarrow \alpha = v, \quad \beta = u \\ \vec{g}^C = \vec{g}(u_C, v_{CTE}), &\quad f^C = f(u_C, v_{CTE}). \end{aligned} \tag{10}$$

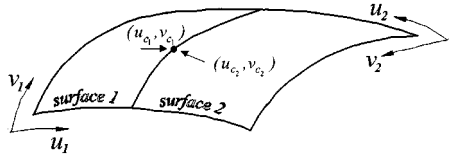

Fig. 3. Boundary critical point located on boundaries that join two parametric surfaces with continuity in their normal vectors.

When a point on a boundary (u_C, v_C) is isolated from neighboring points, its contribution to the PO integral is performed computing the following expression [12], [16]:

$$\vec{I}_B = j(-1)^{\alpha}\frac{\vec{g}^C}{k}e^{jkf^C}\frac{1}{f^C_{\alpha}}\sqrt{\frac{2j\pi}{kf^C_{\beta\beta}}}\,ds^C. \tag{11}$$

The condition for isolation is driven by the parameter υ_α defined as

$$\upsilon_\alpha = |f^C_\alpha|\sqrt{\frac{k}{2|f^C_{\alpha\alpha}|}}. \tag{12}$$

When υ_α is lower than a specific value, the boundary point is coupled with a critical interior point. Coupled points are taken into account by formulating the contribution in terms of a transition function such as the uniform Fresnel integral, $F_\pm$, with the argument υ_α [16]

$$\begin{aligned}\vec{I}_B =& (-1)^{\alpha}\frac{2\vec{g}^C}{k}e^{jkf^C}\sqrt{\frac{j\pi}{f^C_{\beta\beta}|f^C_{\alpha\alpha}|}}\,\mathrm{sign}\,(\mathrm{f}^{\mathrm{C}}_{\alpha})\\ &\cdot \mathrm{sign}\,(\mathrm{f}^{\mathrm{C}}_{\alpha\alpha})\mathrm{F}_{\mathrm{sign}(\mathrm{f}^{\mathrm{C}}_{\alpha\alpha})}(\upsilon_\alpha)\mathrm{e}^{-\mathrm{j}\,\mathrm{sign}(\mathrm{f}^{\mathrm{C}}_{\alpha\alpha})\upsilon^2_\alpha}\,\mathrm{ds}^{\mathrm{C}}\mathrm{F}_{\pm}(\mathrm{x})\\ =& \int_x^{\infty} e^{\pm jt^2}\,dt.\end{aligned} \tag{13}$$

Expression (13) is applied whenever $\upsilon_\alpha \leq 3.0$. When $\upsilon_\alpha > 3.0$, large parameter for the Fresnel integral, the asymptotic formula (11) is employed. Again, some cases have to be approached specifically:

1 A boundary point coincident with an internal critical point, its contribution as a boundary point is discharged because one half of expression (8) accounts for it.

2 Points located at boundaries shared between two Bézier patches with continuity in the normal vector, Fig. 3. Both contributions, one for each surface, cancel each other out.

C. Vertices Points

These are points where the tangent vector to the boundary domain presents discontinuity. In the squared parametric domain, the vertices are obviously located at the four corners with values for (u_V, v_V): (0.0, 0.0), (1.0, 0.0), (0.0, 1.0), (1.0, 1.0). No condition has to be satisfied; vertices points contribute for all radiation directions. If one vertex has been detected previously as a boundary point or as an interior point, its contribution is now discharged.

The same notation is adopted, where now, the superscript ^{V} denotes the particularization for the parametric coordinates of each vertex (u_V, v_V). At this point, the parameters that allow us to switch between the asymptotic and the uniform expressions υ_u and υ_v are checked for each variable u and v

$$\upsilon_u = |f^V_u|\sqrt{\frac{k}{2|f^V_{uu}|}} \quad \upsilon_v = |f^V_v|\sqrt{\frac{k}{2|f^V_{vv}|}}. \tag{14}$$

When $\upsilon_u > 3.0$ and $\upsilon_v > 3.0$, the vertex contribution is [12]

$$\vec{I}_V = -\vec{g}^V e^{jkf^V}\frac{(-1.0)^{u_V+v_V}}{k^2 f^V_u f^V_v}\,ds^V. \tag{15}$$

However, when the parameters are lower than the required limit; in other words, the vertex point is not isolated, the contribution becomes

$$\begin{aligned}\vec{I}_V =& (-1.0)^{u_V+v_V}\frac{2\vec{g}^V}{k}e^{jkf^V}\\ &\cdot\sqrt{\frac{1}{f^V_{uu}f^V_{vv}}}\,\mathrm{sign}\,(\mathrm{f}^{\mathrm{V}}_{\mathrm{u}})\,\mathrm{sign}\,(\mathrm{f}^{\mathrm{V}}_{\mathrm{v}})\mathrm{T}_{\mathrm{u}}\mathrm{T}_{\mathrm{v}}\,\mathrm{ds}^{\mathrm{V}}\\ T_t =& \mathrm{sign}\,(\mathrm{f}^{\mathrm{V}}_{\mathrm{tt}})\mathrm{F}_{\mathrm{sign}(\mathrm{f}^{\mathrm{V}}_{\mathrm{tt}})}(\upsilon_{\mathrm{t}})\mathrm{e}^{-\mathrm{j}\,\mathrm{sign}(\mathrm{f}^{\mathrm{V}}_{\mathrm{tt}})\upsilon^2_{\mathrm{t}}},\quad \mathrm{t}=\mathrm{u},\mathrm{v}.\end{aligned} \tag{16}$$

As the integration domain is $S_{\mathrm{ILLUMINATED}}$, i.e., the illuminated region discrete points (specular, boundary, vertex) should be visible from the source. To prove this fact, Culling's condition $\hat{k}_I \cdot \hat{n}(\vec{r}') \leq 0.0$ is verified. Once each kind of contribution is calculated, the total value of the PO integral for a specific radiation direction becomes from the summation of all the SPM contributions.

We have to keep in mind that the final summation of all contributions yields only to the PO solution for the radiated field. This has been the assumption for the statement of the problem and for the approach followed to reach the final expression for the integral. No diffraction effects are taken into account. For this last task, additional corrections to the PO solution should be considered in terms of the physical theory of diffraction [27], equivalent current method [28], etc.

One of the main premises of the PO approach is to assume current only on the illuminated region of the structure, therefore, the line that splits the structure into shadowed and illuminated regions should be determined and considered as a new boundary of the model. For the automatic determination of the shadow boundary, a classification of surfaces is made according to its visibility from the source point. As result, three groups of surfaces can be obtained: 1) totally illuminated surfaces; 2) completely shadowed surfaces; and 3) partially illuminated surfaces. The shadow boundary determination is performed by the automatic recursive subdivision in halves of the partially illuminated surfaces for both parametric dimensions u and v [29]. The contribution of the boundaries of the resulting illuminated subpatches will approximate the effect of the shadow boundary.

IV. Numerical Results

Comparisons between the numerical and the asymptotic integration of PO currents are shown. All the simulations have been performed in a silicon graphics machine called Power Challenge (size L) and based on R10000 microprocessors with a peak performance for each microprocessor of 380 MFlops.

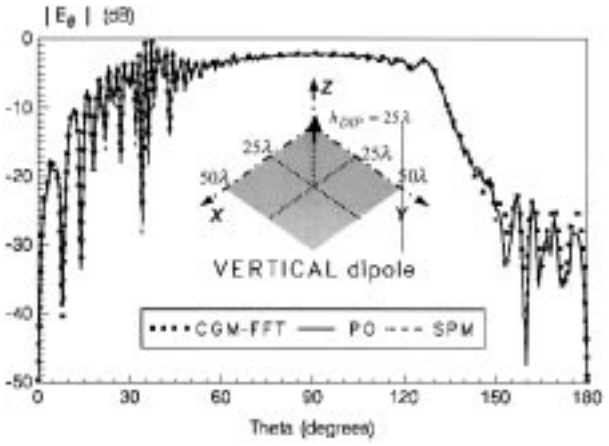

(a)

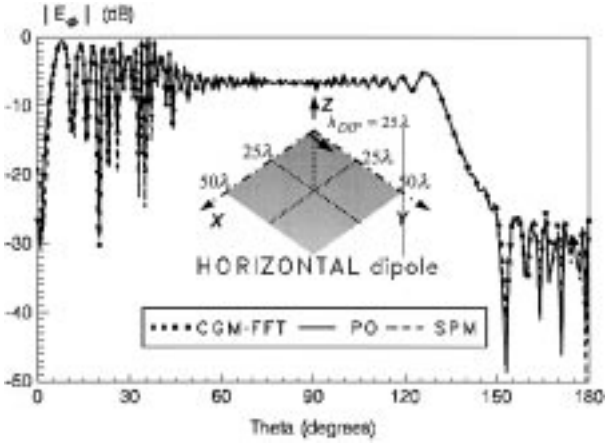

(b)

Fig. 4. Radiation pattern cut for an infinitesimal electric dipole facing a flat surface: (a) vertical dipole, parallel to -axis. (b) horizontal dipole, parallel to -axis.

A. Plate

As a preliminary result, an infinitesimal electric dipole centered and 25λ above a $50\lambda \times 50\lambda$ square plate is analyzed. In [30], the CGM-FFT solves the electric field integral equation (EFIE) for the structure. Fig. 4 displays radiation patterns with comparisons between numerical (continuous line) and asymptotic (dashed line) integration procedures and the rigorous solution from [30] (dotted line). The antenna is vertically oriented with respect to the surface [Fig. 4(a)] or parallel to the facet [Fig. 4(b)]. For both configurations we analyze the radiation pattern cut, $\varphi = 0°$. The efficiency attained is reflected by the computation time. While the numerical integration took 17 min 9 s, the asymptotic integration obtained the solution in only 7 s.

B. Fuselage

A combined curved-planar structure is represented in Fig. 5 with four NURBS surfaces. It resembles the fuselage of an airplane with the flat facets acting as wings. At 3.0 GHz, the electrical size is $120\lambda \times 40\lambda \times 10\lambda$ with a surface area of $3755\lambda^2$. The source is an infinitesimal electric dipole located 10λ over the cylinder with a dipole moment value of $I_0 \cdot l = (1.0, 0°)$. The radiation pattern cut is $\varphi = 90°$, transversal to the cylinder axis, with a sweep in θ angle and displaying the E_θ component is shown in Fig. 6. The continuous-thick line (PO) corresponds to the analysis with numerical integration, the continuous thin-line

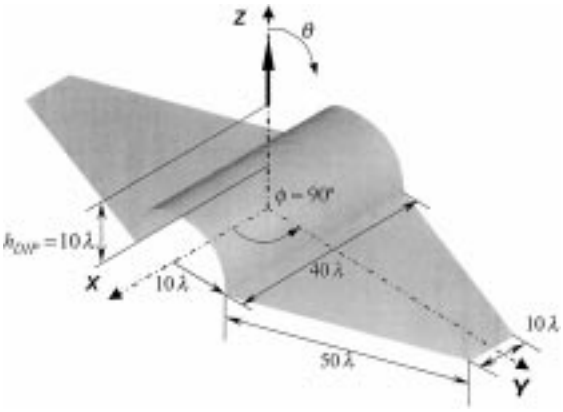

Fig. 5. Fuselage geometry modeled with 4 NURBS surfaces.

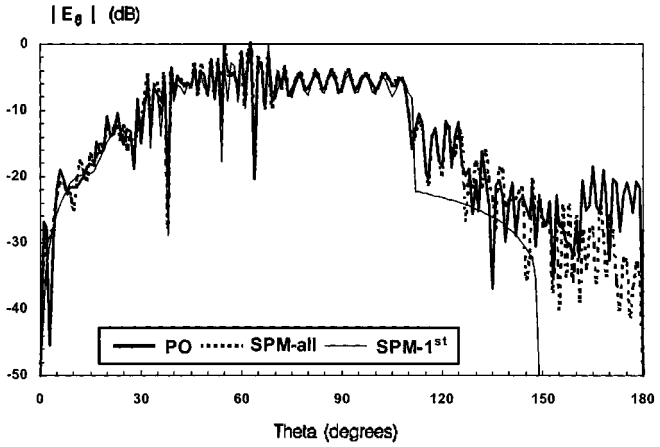

Fig. 6. Radiation pattern cut of an infinitesimal electric dipole over the fuselage. E-component.

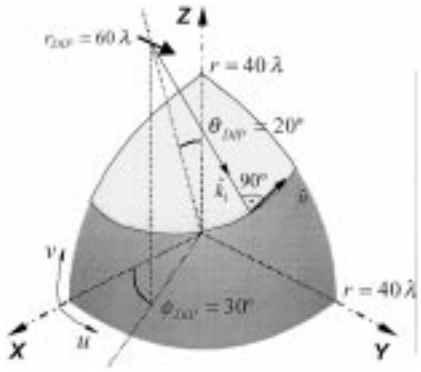

Fig. 7. Shadow boundary on a spherical sector with the source out of the axis.

(SPM-1st) shows the contribution of only the specular points and the dashed thick-line (SPM-all) represents the contribution of the whole set of points (specular, boundary and vertices points). The analysis with numerical integration took 46 min 34 s, whereas, the asymptotic only needs 1 min and 32 s, respectively. Fig. 6 reveals the importance of considering second and third order points contribution. The traditional first order points contribution is not enough to achieve a satisfactory result.

C. Spherical Sector

The effect of the shadow boundary is analyzed for the geometry sketched in Fig. 7. This figure depicts a spherical

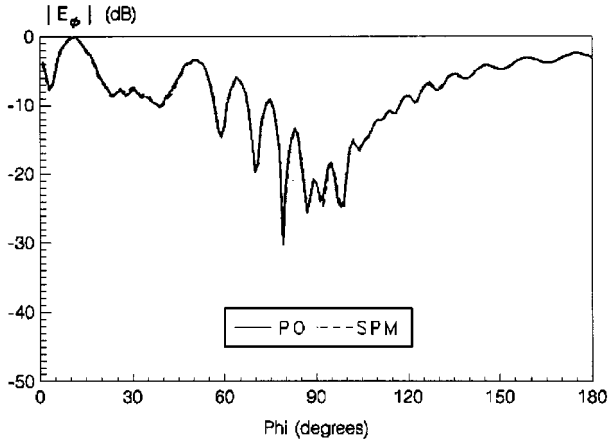

(a)

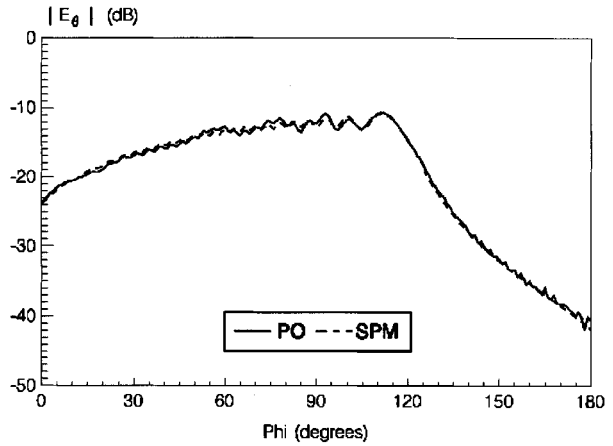

(b)

Fig. 8. Radiation pattern cut of the on-board antenna over the spherical sector. (a) $E\phi$-component. (b) $E\theta$-component.

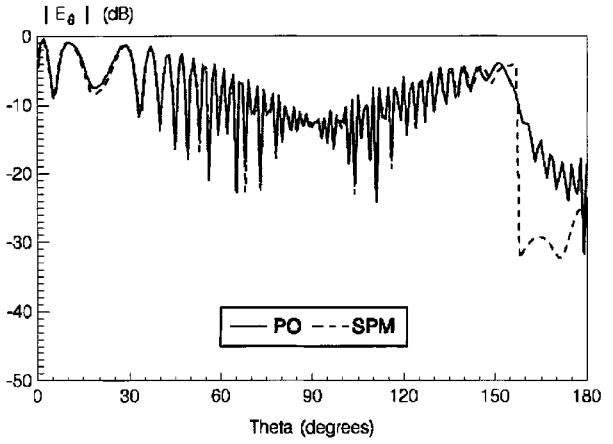

(a)

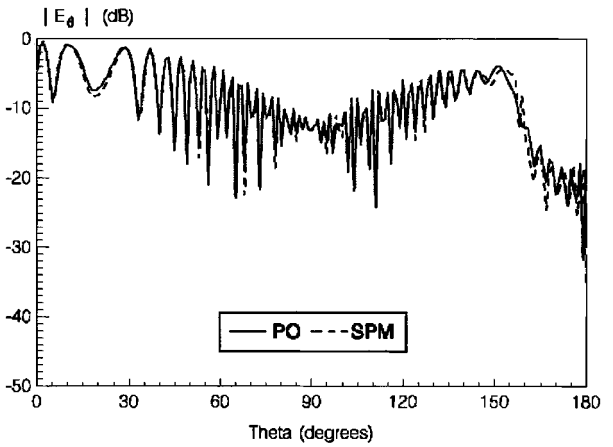

(b)

Fig. 9. Radiation pattern cut 45° for the spherical sector. E-component. (a) Without shadow boundary effect. (b) With shadow boundary effect.

sector with a radius of 40λ. The source is an infinitesimal electric dipole parallel to Y-axis, elevated 20λ over the surface, and displaced from the Z-axis to originate a nonsymmetrical shadow boundary. The angular coordinates of the source are $\theta_{\mathrm{DIP}} = 20°, \varphi_{\mathrm{DIP}} = 30°$, and its dipole moment is $I_0 \cdot l = (1.0, 0°)$.

Results comparing numerical (continuous-line) and asymptotic (dashed-line) integrations for a constant cut $\theta = 90°$ are displayed in Fig. 8. For this radiation pattern, the shadow boundary does not introduce any modification and, therefore, it is not considered. Fig. 9 reveals the effect of the shadow boundary in a constant cut $\varphi = 45°$ for the E_θ component. In Fig. 9(a) only the contribution of specular, vertices, and lateral boundary points is considered. However, in Fig. 9(b), the contribution of the boundary points located over the shadow boundary is also added, giving rise to an improvement for the observation directions with (values greater than 150°). The time for the numerical integration was 20 min 27 s, whereas, the asymptotic one took 5 s without the calculation of the shadow boundary, and 17 s with its computation.

V. Conclusion

The SPM has been applied in the resolution of the integral that accounts for the radiated field associated with antennas mounted on complex geometries. The surface of the body is represented by a set of parametric surfaces, which can be directly defined by the most common geometric modeling tools. Closed-form expressions have been obtained for the contributions of the Stationary Phase Method (specular, boundary and vertices points) in the context of NURBS parametric modeling.

One of the drawbacks is the behavior when the antenna is really quite close to the surface. A hybrid scheme is needed to deal with this feature. The region under the antenna should be treated following a rigorous procedure such as the MFIE, or the EFIE, and the structure far from the antenna point following the asymptotic technique. The causes that bring about the method failure are inherent to the statement of the problem. PO approximation fails because this case represents a typical spherical incidence with no possibility of local plane approximation. Moreover, the premises for the SPM application also fail due to an uneven behavior of the amplitude function (fast variation of the radial component of the incident field due to a source point) and

hence, the principle of phase cancellation is not accomplished. An additional condition to be satisfied by the geometry for an appropriate application of PO approximation is the fact of presenting smooth surfaces with a low number of discontinuities. To deal with such discontinuities, an EM complement such as PTD or the method of equivalent currents should be included. An additional contribution due to the effect of the creeping wave on the shadow region should also be added, this effect could be considered through the introduction of the Fock wave [31]. Another point of further research would be the improvement of the transition function. This function gives rise to a uniform formulation for the case of a first order stationary phase point approaching a boundary of the integration domain. In literature, this problem is considered difficult [6], [21] and no simple solution has yet been found. Finally, this work represents an efficient component in order to be introduced in a more complex computational tool able to analyze, in a complete and rigorous way, the effect on arbitrary structures on the radiation pattern of boarded antennas.

ACKNOWLEDGMENT

The authors wish to thank Professor P. H. Pathak for his helpful comments on this study about high-frequency techniques.

REFERENCES

[1] G. Farin, *Curves and Surfaces for Computer Aided Geometric Design, A Practical Guide*. New York: Academic , 1988.
[2] R. F. Harrington, *Time-Harmonic Electromagnetic Fields*. New York: McGraw-Hill, 1961.
[3] C. A. Balanis, *Advanced Engineering Electromagnetics*. New York: Wiley, 1989.
[4] J. A. Shifflett, "CADDRAD: A physical optics radar/radome analysis code for arbitrary 3D geometries," *IEEE Antennas Propagat.*, vol. 39, pp. 73–79, Dec. 1997.
[5] W. H. Press, B. P. Flannery, S. A. Teukolsky, and W. T. Vetterling, *Numerical Recipes*. Cambridge, U.K.: Cambridge Univ. Press, 1987.
[6] N. Chako, "Asymptotic expansions of double and multiple integrals occuring in diffraction theory," *IMA J. Appl. Math.* , vol. 1, pp. 372–422, 1965.
[7] A. C. Ludwig, "Computation of radiation patterns involving numerical double integration," *IEEE Trans. Antennas Propagat.*, vol. AP-16, pp. 767–769, Nov. 1968.
[8] L. B. Felsen and N. Marcuvitz, *Radiation and Scattering of Waves*. Englewood Cliffs, NJ: Prentice-Hall, 1973.
[9] D. S. Jones and M. Kline, "Asymptotic expansion of multiple integrals and the method of stationary phase," *J. Math. Phys.*, vol. 37, pp. 1–28, 1958.
[10] M. Born and E. Wolf, *Principles of Optics*. London: Pergamon, 1975.
[11] L. Sirovich, *Techniques of Asymptotic Analysis*. New York: Springer-Verlag, 1971.
[12] J. C. Cooke, "Stationary phase in two dimensions," *IMA J. Appl. Math.*, vol. 29, pp. 25–37, 1982.
[13] N. Bleistein and R. A. Handelsman, "Uniform asymptotic expansions of double integrals," *J. Math. Anal. Appl.*, vol. 27, pp. 434–453, 1969.
[14] ——, *Asymptotic Expansions of Integrals*. New York: Dover , 1975.
[15] J. P. McClure and R. Wong, "Two-dimensional stationary phase approximation: Stationary point at a corner," *SIAM J. Math. Anal.*, vol. 22, pp. 500–523, Mar. 1991.
[16] G. L. James, *Geometrical Theory of Diffraction for Electromagnetic Waves*. Stevenage, U.K.: Peregrinus, 1980.
[17] R. G. Kouyoumjiam and P. H. Pathak, "A uniform geometrical theory of diffraction for an edge in a perfectly conducting surface," *Proc. IEEE*, vol. 62, pp. 1448–1461, Nov. 1974.
[18] W. H. Ierley and H. Zucker, "A stationary phase method for the computation of the far field of open cassegrain antennas," *Bell Syst. Tech. J.*, vol. 49, pp. 431–454, Mar. 1970.
[19] C. A. Siller, Jr., "Evaluation of the radiation integral in terms of endpoint contributions," *IEEE Trans. Antennas Propagat.*, vol. AP-23, pp. 743–745, Sept. 1975.
[20] H. Ikuno, "Calculation of far-scattered fields by the method of stationary phase," *IEEE Trans. Antennas Propagat.*, vol. AP-27, pp. 199–202, Mar. 1979.
[21] H. Ikuno and M. Nishimoto, "Calculation of transfer functions of three-dimensional indented objects by the physical optics approximation combined with the method of the stationary phase," *IEEE Trans. Antennas Propagat.*, vol. 39, pp. 585–590, May 1991.
[22] H. Nakano, S. R. Kerner, and N. G. Alexopoulos, "The moment method solution for printed wire antennas of arbitrary configuration," *IEEE Trans. Antennas Propagat.*, vol. AP-36, pp. 1667–1674, Dec. 1988.
[23] J. Pérez and M. F. Cátedra, "Application of physical optics to the RCS computation of bodies modeled with NURBS surfaces," *IEEE Trans. Antennas Propagat.*, vol. 42, pp. 1404–1411, Oct. 1994.
[24] G. T. Ruck, *Radar Cross Section Handbook*. New York: Plenum Press, 1970.
[25] S.-W. Lee, P. Cramer, Jr., K. Woo, and Y. Rahmat-Samii, "Diffraction by an arbitrary subreflector: GTD solution," *IEEE Trans. Antennas Propagat.*, vol. AP-27, pp. 305–316, May 1979.
[26] J. Pérez, J. A. Sáiz, O. M. Conde, R. P. Torres, and M. F. Cátedra, "Analysis of antennas on board arbitrary structures modeled by NURBS surfaces," *IEEE Trans. Antennas Propagat.*, vol. 45, pp. 1045–1053, June 1997.
[27] P. Y. Ufimtsev, "Elementary edge waves and the physical theory of diffraction," *Electromagnetics*, vol. 11, pp. 127–160, Apr.–June 1991.
[28] A. Michaeli, "Elimination of infinities in equivalent edge currents, part I: Fringe current components," *IEEE Trans. Antennas Propagat.*, vol. 34, pp. 912–918, July 1986.
[29] O. M. Conde, "Contribución al Estudio del Comportamiento de Antenas Embarcadas Empleando Técnicas Integrales y Asintóticas," Ph.D. thesis, University of Cantabria, Spain, July 1999.
[30] M. F. Cátedra, J. G. Cuevas, and L. Nuño, "A scheme to analyze conducting plates of resonant size using the conjugate-gradient method and the fast fourier transform," *IEEE Trans. Antennas Propagat.*, vol. 36, pp. 1744–1752, Dec. 1988.
[31] C. W. Chuang, "An asymptotic solution for currents in the penumbra region with discontinuity in curvature," *IEEE Trans. Antennas Propagat.*, vol. AP-34, pp. 728–732, May 1986.

Olga M. Conde was born in Cantabria, Spain, in 1970. She received the Engineering and Ph.D. degrees in Telecommunications from the University of Cantabria, Santander, Spain, in 1994 and 1999, respectively.

In October, 1999, she joined the Photonics Engineering Group, conducting academic and research on optical communications at the University of Cantabria. From 1994 to 1999, her research focused on the development of numerical methods for the electromagnetic and optical fields, the analysis of on-board antennas and satellite communications systems. Her current research interests include the development of optical sensors for the detection and monitoring of dangerous gaseous compounds in urban or industrial environments.

Jesús Pérez Arriaga received the M.S. and Ph.D. degrees in applied physics from the University of Cantabria, Cantabria, Spain.

In 1989 he joined the Radiocommunication and Signal Processing Department of the Polytechnic University of Madrid, Spain, as a research assistant. From 1990 to 1992, he joined the Electronics Department, University of Cantabria, also as a research assistant. In 1993 he joined the faculty of the University of Cantabria, as an assistant professor in the Electronic Department. In October 1998, he joined the University of Alcalá, Madrid, Spain, as an assistant professor. He has participated in more than 20 research projects related to RCS computation, performed analysis of on-board antennas and radiopropagation in mobile communications. He is author of 10 journal publications, coauthor of *Cell Planning for Wireless Communications* Norwood, MA: Artech House, 1999, and more than 25 conference contributions at international symposia. His research interests include high-frequency methods in electromagnetic radiation and scattering and mobile communications.

Manuel Felipe Cátedra received the M.S. and Ph.D. degrees in Telecommunications Engineering from the Polytechnic University of Madrid, Madrid, Spain, in 1977 and 1982, respectively.

In 1976, he joined the Radiocommunication and Signal Processing Department, University of Madrid, as a research and faculty member. In 1989, he joined the University of Cantabria, Spain as a professor. In 1998, he joined the University of Alcalá, Madrid, Spain, where he is currently a Professor.

His publishing record includes 35 journal articles, ten book chapters, and author or coauthor of two books*The CG-FFT Method Applications of Signal Processing techniques to Electromagnetics*, Norwood, MA: Artech House, 1995, *Cell Planning for Wireless Communications* Norwood, MA: Artech House, 1999, and has nearly 100 presentations in International Symposia. His extensive research includes over 25 projects solving problems of Electromagnetic Compatibility in Radio and Telecommunication Equipment, Antennas, Microwave Components and Radar Cross Section and Mobile Communications. He has developed and applied CAD tools for radio-equipment systems such as Navy-ships, aircraft, helicopters, satellites, the main contractors being Spanish or European Institutions such as CASA, ALCATEL, DASA, SAAB, INTA, BAZAN, the Spanish Defence Department and the French company MATRA. He is working now on projects for Telefonica (the largest Spanish telecommunication company) to develop computer tools for propagation analyzes in microcells and indoor cells.